Comparative assessment of a new nonempirical density functional: Molecules and hydrogen-bonded complexes

Viktor N. Staroverov[a)] and Gustavo E. Scuseria
Department of Chemistry, Rice University, Houston, Texas 77005

Jianmin Tao and John P. Perdew
Department of Physics and Quantum Theory Group, Tulane University, New Orleans, Louisiana 70118

A comprehensive study is undertaken to assess the nonempirical meta-generalized gradient approximation (MGGA) of Tao, Perdew, Staroverov, and Scuseria (TPSS) against 14 common exchange-correlation energy functionals. Principal results are presented in the form of statistical summaries of deviations from experiment for the G3/99 test set (223 enthalpies of formation, 86 ionization potentials, 58 electron affinities, 8 proton affinities) and three additional test sets involving 96 bond lengths, 82 harmonic vibrational frequencies, and 10 hydrogen-bonded complexes, all computed using the $6\text{-}311++\text{G}(3df,3pd)$ basis. The TPSS functional matches, or exceeds in accuracy all prior nonempirical constructions and, unlike semiempirical functionals, consistently provides a high-quality description of diverse systems and properties. The computational cost of self-consistent MGGA is comparable to that of ordinary GGA, and exact exchange (unavailable in some codes) is not required. A one-parameter global hybrid version of the TPSS functional is introduced and shown to give further improvement for most properties. © *2003 American Institute of Physics.* [DOI: 10.1063/1.1626543]

I. INTRODUCTION

Development of approximate exchange-correlation energy functionals for Kohn–Sham (KS) density functional theory (DFT)[1–4] embodies two different philosophies. The first assumes that since there is no hope of writing down the exact universal functional, the best strategy is to make a reasonable guess in parametric form and optimize it by fitting to a set of experimental data. This approach has produced the most popular density functionals for atoms and molecules, BLYP[5,6] and B3LYP.[7] Further improvements along this line rely on increasing the number of empirical parameters,[8,9] generalizing the fitting procedure beyond energetic data,[10,11] and introducing new variables like the noninteracting kinetic energy density.[12–14] For a given training set, the functional optimization is actually quite systematic.[15] Unfortunately, better fits are not necessarily closer approximations to the universal functional, and even the best semiempirical constructions can fail outside their training sets.

The second approach espouses the idea that approximate functionals should be developed from first principles by incorporating known exact constraints, and that if enough constraints are satisfied, all physical properties will come out right by themselves. In practice, in order to impose more and more exact constraints on a functional $E_{\text{xc}}[\rho_\alpha,\rho_\beta]$, it becomes necessary to expand the list of its local ingredients beyond the electron density to include other quantities constructed from the KS orbitals and their derivatives. The hierarchy of density functional approximations organized by the type of these ingredients has been pictured as "Jacob's lad-der" rising from the "Hartree world" to the "chemical accuracy heaven." [16,17] Since the practice of adding new ingredients is also found in the arsenal of the semiempirical method, the ladder classification applies to both types of functionals.

Within the nonempirical approach, capacities of the first and second rungs of Jacob's ladder have been effectively exhausted by, respectively, the local spin-density approximation (LSDA)[1,18,19] and the Perdew–Burke–Ernzerhof (PBE) generalized gradient approximation (GGA).[20,21] Recent developments concentrate on the third rung, where the list of GGA ingredients [electron density $\rho_\sigma(\mathbf{r})$ and its gradient] is expanded to include the kinetic energy density of the occupied KS orbitals, $\tau_\sigma(\mathbf{r})=\frac{1}{2}\Sigma_i|\nabla\phi_i^\sigma(\mathbf{r})|^2$, with $\sigma=\alpha,\beta$, and/or Laplacians of the density. Density functionals of this type, called meta-GGA (MGGA), have been proposed by Perdew,[22] Ghosh and Parr,[23] Becke and Roussel,[24] Van Voorhis and Scuseria (VSXC),[12] Schmider and Becke,[13] Filatov and Thiel,[25] Perdew, Kurth, Zupan, and Blaha (PKZB),[26] Krieger *et al.*,[27] Proynov *et al.*,[28] and others. Most of these approximations were examined on a comparative basis by Kurth *et al.*[29]

The PKZB functional adheres to the principles of the nonempirical philosophy more strictly than other published MGGAs. In addition to all the exact constraints inherited from PBE, including the correct second-order gradient expansion for correlation, it reproduces the correct gradient expansion of the exchange energy to second order in ∇, as well as two of the three fourth-order terms. An essential feature of the PKZB correlation is that it is self-interaction free, that is, vanishes for one-electron densities. (The trick makes use of the fact that in any one-electron system $\tau_\sigma=\tau_\sigma^W$, where τ_σ^W

[a)]Electronic mail: vstarove@rice.edu

12129

$=|\nabla\rho_\sigma|^2/8\rho_\sigma$ is the Weizsäcker kinetic energy density). However, the PKZB functional does have one empirical parameter in the exchange component and, despite a very good performance for atomization energies,[30] is inferior to PBE for equilibrium bond lengths and vibrational frequencies,[30] as well as dissociation energies and geometries of hydrogen-bonded complexes.[31] These concerns prompted us recently to revise the PKZB approximation and propose an improved MGGA functional,[32] named TPSS (Tao, Perdew, Staroverov, and Scuseria). The original TPSS paper focused on formal development. In this work, we present an extensive assessment of TPSS as a new functional for molecular electronic structure calculations and introduce its one-parameter hybrid version.

A general-purpose density functional should work for solids and solid surfaces as well as for atoms and molecules. Semiempirical functionals fitted to thermochemical data can fail badly for solids and surfaces,[29] but our nonempirical TPSS functional works well for such systems, as shown in Refs. 32 and 33. In particular, surface energies appear to be given accurately by the TPSS MGGA and its hybrid. Presumably, these functionals should also work well for clusters and for molecules[34] or chemical reactions at surfaces.

II. THE TPSS AND HYBRID TPSS FUNCTIONALS

TPSS exchange and correlation have the same local ingredients as PKZB. The exchange part of the TPSS functional has the traditional form of a gradient-enhanced LSDA exchange,

$$
\begin{aligned}
&E_x^{TPSS}[\rho_\alpha,\rho_\beta] \\
&= \sum_{\sigma=\alpha,\beta} \int \rho_\sigma \epsilon_x^{LSDA}(\rho_\sigma) F_x(\rho_\sigma,\nabla\rho_\sigma,\tau_\sigma)\,d\mathbf{r},
\end{aligned}
\tag{1}
$$

where $\epsilon_x^{LSDA}(\rho_\sigma) = -(3/4)(6/\pi)^{1/3}\rho_\sigma^{1/3}$ is the σ component of the LSDA exchange energy per particle, and $F_x(\rho_\sigma,\nabla\rho_\sigma,\tau_\sigma)$ is a relatively complicated enhancement factor which reduces to 1 for a uniform density and preserves the LSDA exchangelike scaling. In PBE and PKZB, the enhancement factors are such that the corresponding exchange potentials $v_x^\sigma(\mathbf{r})$ diverge at the nuclei (see Fig. 1). In the case of PKZB, the divergence of $v_x^\sigma(\mathbf{r})$ is manifested in overstretched bond lengths. This problem was addressed in the TPSS approximation by requiring that $v_x^\sigma(\mathbf{r})$ be finite at the nucleus whenever $\tau_\sigma^W=\tau_\sigma$, which covers all iso-orbital (i.e., one- and spin-compensated two-electron) densities. Iso-orbital densities are crucial because they represent two fundamental models of quantum chemistry—the hydrogen atom and chemical bond. In effect, the new constraint eliminates the divergence for *all* realistic many-electron systems, since the electron density near the nucleus is dominated by the 1*s* orbital, so that $\tau_\sigma\to\tau_\sigma^W$. Chronologically, this was the last and key constraint that made it possible to get good atomization energies *and* bond lengths from a nonempirical MGGA. The improvement is probably due not so much to the behavior of the exchange potential in the nearly iso-orbital region around the nucleus as to its behavior in nearly iso-orbital valence-electron regions. Figure 1 also shows that
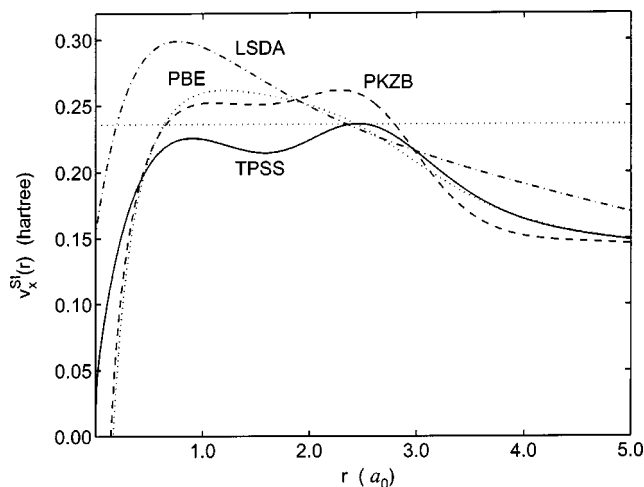

FIG. 1. Exchange-only self-interaction potentials as functions of the distance from the nucleus. The potential is defined as $v_x^{SI}(\mathbf{r})=v_x^\alpha([\rho_\alpha,0];\mathbf{r}) + \int d\mathbf{r}'\,\rho_\alpha(\mathbf{r}')/|\mathbf{r}'-\mathbf{r}|$ and computed on the exact density of the H atom. The correct $\mathbf{r}$-independent result is shown by the horizontal dotted line at $\frac{1}{2}(I-A)=0.2360\,E_h$, where I is the ionization potential and A is the electron affinity of the H atom. A spurious $1/r$ divergence of v_x^α at the nucleus appears when we pass from LSDA to PBE or PKZB, but is removed in TPSS. The correct result is the exact self-interaction potential averaged over the discontinuity (Ref. 73) from 0 to $I-A$ that occurs as the electron number N increases through the integer 1.

although the TPSS exchange is not completely free from spurious self-interaction even for one-electron densities, it is a step forward from PKZB.

The correlation part of TPSS is not separable into spin-up and spin-down components:

$$
E_c^{TPSS}[\rho_\alpha,\rho_\beta] = \int \rho\,\epsilon_c^{revPKZB}\left[1+d\left(\frac{\tau_W}{\tau}\right)^3\epsilon_c^{revPKZB}\right]d\mathbf{r}.
\tag{2}
$$

Here $\rho=\rho_\alpha+\rho_\beta$, $\tau=\tau_\alpha+\tau_\beta$, $\tau_W=|\nabla\rho|^2/8\rho$, $\epsilon_c^{revPKZB}(\rho_\alpha,\rho_\beta,\nabla\rho_\alpha,\nabla\rho_\beta,\tau)$ is the revised PKZB correlation energy per particle, and d is a nonempirical constant. In a monovalent atoms like Li (see Fig. 2), LSDA and PBE have a spurious self-correlation in the one-electron-like valence region ($r>2\,a_0$), which is removed in PKZB and TPSS. Note, however, that the PKZB self-correlation correction improperly enhances correlation energy density in the intershell region ($r\approx 2\,a_0$), a flaw that is eliminated in the TPSS MGGA. The build-up effect is reflected in the correlation energy of the Li atom (in hartree): -0.151 (LSDA), -0.051 (PBE), -0.054 (PKZB), -0.049 (TPSS), and -0.046 (exact).

A global hybrid form of the new MGGA functional is obtained by mixing TPSS with exact exchange:

$$
E_{xc}^{TPSSh} = aE_x^{exact}+(1-a)E_x^{TPSS}+E_c^{TPSS}.
\tag{3}
$$

The TPSSh functional has one empirical parameter whose optimal value $a=0.10$ was determined by minimizing the mean absolute deviation in the enthalpies of formation of 223 G3/99 molecules using the 6-311++G(3*df*,3*pd*) basis (compare with the PKZB hybrid scheme[30]). TPSSh satisfies precisely the same exact constraints as the original TPSS. The fact that the value of a is often (but not always[13])
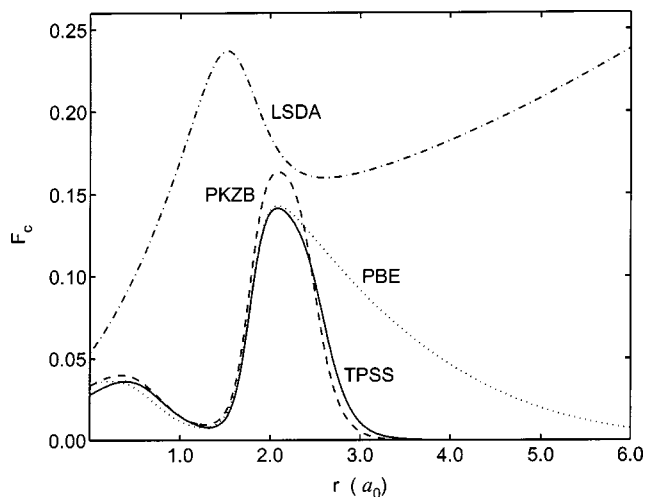
FIG. 2. Correlation enhancement factors for the Li atom as functions of the distance from the nucleus. The factor is defined as $F_c(\mathbf{r}) = \epsilon_c(\mathbf{r})/\epsilon_x^{LDA}(\mathbf{r})$, where $\epsilon_c(\mathbf{r})$ is the correlation energy per electron and $\epsilon_x^{LDA}(\mathbf{r}) = -(3/4) \times [3\rho(\mathbf{r})/\pi]^{1/3}$ is the exchange energy per electron for the unpolarized uniform electron gas. By Eq. (2), $\epsilon_c^{TPSS} = \epsilon_c^{revPKZB}[1 + d\epsilon_c^{revPKZB}(\tau_W/\tau)^3]$. The density $\rho(\mathbf{r})$ is from the Hartree–Fock wave function of Clementi and Roetti (Ref. 74). The PKZB enhancement factor is slightly negative ($|F_c| < 10^{-4}$) in the tail region ($r > 4 \, a_0$), where the relative spin polarization $\zeta = (\rho_\alpha - \rho_\beta)/\rho$ approaches 1, while the other enhancement factors are non-negative for all possible electron densities.

smaller for hybrid MGGAs than for hybrid GGAs (where it varies from 0.16 to 0.29[35]) indicates that MGGAs can have a more realistic dependence on the coupling constant λ of the adiabatic connection formula.

III. METHODOLOGY

The objective of this work is to present a comprehensive and reliable assessment of the TPSS functional for atoms and molecules. To meet the former requirement, we consider a variety of energetic and structural properties including enthalpies of formation, ionization potentials, electron and proton affinities, bond lengths, and vibrational frequencies. In each case, the performance of TPSS is compared to that of 14 common density functionals: LSDA (using the Perdew–Wang parametrization[19] of the uniform gas correlation energy), PW91[36,37] and PBE (nonempirical GGAs with different derivations but very similar performance), BLYP, BPW91, BP86,[38] HCTH/407,[11] OLYP[39] (semiempirical GGAs), B3LYP, B3PW91,[40] B3P86,[41] PBE0[42,43] (hybrid GGAs), VSXC, and PKZB (semiempirical MGGAs), plus the Hartree–Fock (HF) approximation. As usual, calculations on open shells are spin-unrestricted. The only nonempirical hybrid functional in this list is PBE0, whose exact-exchange mixing coefficient is fixed by a theoretical estimate.[44] The semiempirical functionals have as many as 15 (HCTH/407) or 21 (VSXC) empirical parameters. The functionals correct in the uniform density limit, and to that extent suitable for solids, are LSDA, PW91, PBE, BPW91, BP86, B3PW91, PBE0, PKZB, TPSS, and TPSSh.

In order for the assessment to be reliable, calculations should be performed with a sufficiently large basis set and compared to well-established experimental data. We chose the $6\text{-}311++\text{G}(3df,3pd)$ basis, which is larger than most basis sets used in DFT. Although not especially close to the complete basis set limit, it represents a reasonable model chemistry.[45,46] The choice of experimental reference data is discussed in the following.

The TPSS functional was implemented in a developmental version of the GAUSSIAN program.[47] Since $\tau(\mathbf{r})$ is not an explicit functional of $\rho(\mathbf{r})$, the TPSS exchange-correlation potential, $v_{xc}^\sigma(\mathbf{r}) = \delta E_{xc}/\delta\rho_\sigma(\mathbf{r})$, cannot be calculated directly. To circumvent this difficulty, matrix elements of $v_{xc}^\sigma(\mathbf{r})$, gradients, and Hessians of the TPSS exchange-correlation energy were evaluated by the method of Neumann et al.,[48] using analytical derivatives and the "UltraFine" integration grid. This method consists in making the total energy stationary with respect to orbital variations and yields a differential operator rather than the correct local (multiplicative) KS potential (see also Ref. 49). Total energies obtained by this means are close to the proper KS result for most practical purposes. A similar approach is routinely used for hybrid density functionals, except that the Hartree–Fock potential there is nonlocal. Alternatively, a MGGA KS potential could be found by the optimized effective potential method.[50]

Because the orbitals are available in any Kohn–Sham-like procedure, calculations with MGGA functionals are not much slower than with GGAs. On most machines, the increase in computation time is roughly 20% and even less for larger molecules.

For each property/functional combination, we report only a statistical summary of deviations of calculated values from experiment. This includes the mean error (ME), the mean absolute error (MAE), and the largest positive and negative deviations within the set. Throughout this work, we use the following sign convention: deviation=theory −experiment. For consistency, we performed our own calculations with all 14 reference functionals rather than attempting to extract relevant data from the literature. In fact, nearly all of our results are reported for the first time. Supplementary tables showing deviations of calculated properties for individual species are available through the EPAPS depository.[51]

IV. THERMOCHEMICAL PROPERTIES

The thermochemical test set of Curtiss et al.[52–56] was initially intended as a proving ground for composite Gaussian-n ($n=1-3$) theories.[52,57,58] The most recent modification of this set, known as G3/99, includes 223 standard enthalpies of formation (we did not delete the COF_2 molecule, as recommended by Curtiss et al.[56]), 88 ionization potentials, 58 electron affinities, and 8 proton affinities. Only the first- and second-row elements ($Z \leqslant 18$) are represented. For historical reasons, the 223 enthalpies of formation are sometimes grouped into three subsets which we will designate G3-1, G3-2, and G3-3. These subsets represent three stages in the development of the G3/99 set and comprise 55, 93, and 75 molecules, respectively. The G3-1 and G3-2 sub-

TABLE I. Summary of deviations from experiment of standard enthalpies of formation ($\Delta_f H^\circ_{298}$) for the G3/99 test set computed with various methods using the $6\text{-}311++\text{G}(3df,3pd)$ basis set. The geometries and zero-point energies were obtained at the B3LYP/6-31G($2df,p$) level using a frequency scale factor of 0.9854. All values are in kcal/mol. Error=theory−experiment. The mean experimental atomization energies (ΣD_0) for the G2/97 and G3-3 sets are 478 and ~1180 kcal/mol, respectively.

Method	G2/97 (148)				G3-3 (75)				G3/99 (223)	
	ME	MAE	Max (+)	Max (−)	ME	MAE	Max (+)	Max (−)	ME	MAE
HF	148.27	148.27	344.1 (C_5H_5N)	−0.5 (BeH)	336.37	336.37	582.2 (C_8H_{18})	None	211.53	211.54
LSDA	−83.71	83.71	0.4 (Li_2)	−207.7 (C_6H_6)	−197.11	197.11	None	−347.5 (azulene)	−121.85	121.85
BLYP	−0.56	7.27	24.2 ($SiCl_4$)	−28.1 (NO_2)	12.42	13.88	41.0 (C_8H_{18})	−11.0 ($C_4H_4N_2$)	3.81	9.49
BPW91	−5.40	8.00	16.5 (SiF_4)	−32.4 (NO_2)	−4.97	11.08	22.4 [$Si(CH_3)_4$]	−28.0 (azulene)	−5.26	9.04
BP86	−19.85	20.11	7.1 (SiF_4)	−48.7 (C_5H_5N)	−38.61	38.61	None	−72.7 (azulene)	−26.16	26.33
PW91	−17.20	17.69	7.5 (Si_2H_6)	−52.7 (C_2F_4)	−35.25	35.25	None	−81.1 (azulene)	−23.27	23.59
PBE	−16.07	16.87	10.8 (Si_2H_6)	−50.5 (C_2F_4)	−32.77	32.77	None	−79.7 (azulene)	−21.69	22.22
HCTH	−0.61	5.64	16.5 ($SiCl_4$)	−28.0 (C_2F_4)	6.38	10.18	27.5 [$Si(CH_3)_4$]	−22.2 (C_2F_6)	1.74	7.17
OLYP	−1.86	4.84	27.0 (SiF_4)	−23.5 (NO_2)	6.41	7.91	20.9 [$Si(CH_3)_4$]	−11.0 (CF_3)	0.92	5.88
B3LYP	1.12	3.14	20.1 (SiF_4)	−8.1 (BeH)	8.23	8.44	20.8 (SF_6)	−4.9 ($C_4H_4N_2$)	3.51	4.93
B3PW91	−1.42	3.40	21.6 (SiF_4)	−12.8 (C_2F_4)	−2.54	4.87	17.0 (PF_5)	−17.0 (naphthalene)	−1.80	3.90
B3P86	−17.91	18.16	7.5 (SiF_4)	−48.1 (C_5H_8)	−41.89	41.89	None	−79.2 (C_8H_{18})	−25.98	26.14
PBE0	−2.42	4.87	21.3 (SiF_4)	−19.8 (C_5H_5N)	−9.28	10.20	14.5 (PF_5)	−35.6 (naphthalene)	−4.73	6.66
VSXC	−0.51	2.81	8.2 (N_2H_4)	−11.5 (CS_2)	1.97	4.74	12.0 (C_8H_{18})	−8.7 (C_6H_5)	0.32	3.46
PKZB	0.57	4.83	39.8 (SiF_4)	−18.0 (NO_2)	10.59	11.24	35.4 (PF_5)	−11.0 (P_4)	3.94	6.98
TPSS	−5.21	5.98	16.2 (SiF_4)	−22.9 (ClF_3)	−5.19	5.48	7.5 (PF_5)	−12.8 (S_2Cl_2)	−5.20	5.81
TPSSh	−1.38	4.19	22.0 (SiF_4)	−18.0 (Si_2H_6)	0.16	3.33	16.2 (PF_5)	−6.6 (C_8H_{18})	−0.86	3.90

sets together form the G2/97 set (148). The G3-3 extension includes larger organic molecules and several problematic inorganic species.

As a continuously updated compilation of critically evaluated experimental data, the G2/97 and G3/99 sets are now widely used for the assessment and calibration of density functional methods. Single-point calculations of the molecules included in these sets were originally performed at the MP2(full)/6-31G* (second order Møller–Plesset) geometries using scaled HF/6-31G* frequencies. Subsequently it was demonstrated[59–61] that B3LYP geometries and frequencies are a slightly better alternative to the MP2/HF combination. In Ref. 32 we employed the MP2/HF geometries/frequencies, but in this work we adopt the procedure of the G3X theory,[62] which uses the equilibrium B3LYP/6-31G($2df,p$) geometries in combination with the B3LYP/6-31G($2df,p$) zero-point energies (ZPE) and thermal corrections obtained with a frequency scale factor of 0.9854. The G3/99 test set generated at this level of theory is denoted G3//B32df.[62] We have examined the effect of full geometry relaxation on G3 proton affinities and found it to be negligible.

A. Standard enthalpies of formation

The most natural measure of chemical binding is the molecular atomization energy (reported as ΣD_0 or ZPE-subtracted ΣD_e). However, in assessments of thermochemical accuracy of quantum chemical methods, standard enthalpies of formation ($\Delta_f H^\circ_{298}$) are now preferred because: (i) experimental $\Delta_f H^\circ_{298}$ are more readily available than experimental ΣD_0; (ii) unlike estimates of ΣD_e, enthalpies of formation are directly observable quantities. Loosely speaking, the error in the enthalpy of formation (as we calculate it) is *minus* the error in the atomization energy.

In this work, standard enthalpies of formation were computed from total atomic and molecular energies using the experimental atomic data and methodology described by Curtiss *et al.*[54] For ease of comparison with earlier studies, we report separate G2/97 and G3-3 statistics.

Based on the G2/97 results shown in Table I, the TPSS functional (MAE=6.0 kcal/mol) appears to be less accurate than PKZB (4.8 kcal/mol). A 10% contribution from exact exchange in the TPSS hybrid (TPSSh) brings down the MAE to 4.2 kcal/mol. G3-3 results, however, suggest a different story. It is well known that errors in enthalpies of formation tend to increase with molecular size. As seen from Table I, the MAE of all functionals predating TPSS increases significantly from the G2/97 to G3-3 set, in some cases more than by a factor of 2. For example, the MAE of PKZB for the G3-3 set is 11.2 kcal/mol. TPSS and TPSSh are the only functionals for which the MAE actually decreases (from 6.0 to 5.5 kcal/mol and from 4.2 to 3.3 kcal/mol, respectively). For TPSS, this remarkable effect has been first observed by Csonka *et al.*[63] in non-self-consistent 6-311G(d,p) post-PBE calculations of 50 organic molecules picked from the G3-3 set. The present study employing self-consistent energies, a larger basis, and the full G3-3 test set substantiates their conclusion. Considering the entire G3/99 set, we see that the TPSS functional (MAE=5.8 kcal/mol) is actually more accurate than PKZB (7.0 kcal/mol).

Overall, the results obtained with TPSS and TPSSh are very encouraging. Performance of these new functionals for enthalpies of formation is comparable to that of the best semiempirical approximations: B3LYP, B3PW91, and VSXC. Although the highest accuracy for the full G3/99 set is achieved by VSXC (MAE=3.5 kcal/mol), TPSSh is unrivaled within the G3-3 set, where it outperforms by far B3LYP and, to a lesser extent, B3PW91 and VSXC. The TPSS functional is also much more successful than B3LYP

J. Chem. Phys., Vol. 119, No. 23, 15 December 2003

Nonempirical DFT   12133

TABLE II. Summary of deviations from experiment of ionization potentials (IP) of the G3/99 test set (86 species) computed using the 6-311++G($3df,3pd$) basis. The geometries and zero-point energies were obtained at the B3LYP/6-31G($2df,p$) level using a frequency scale factor of 0.9854. All values are in eV. Error=theory−experiment. The mean experimental IP is 10.89 eV.

Method	ME	MAE	Max (+)	Max (−)
HF	−0.958	1.028	2.60 (CN)	−1.82 (Ne)
LSDA	0.048	0.232	1.18 (CN)	−0.69 (BCl_3)
BLYP	−0.191	0.286	1.03 (CN)	−1.06 (BF_3)
BPW91	−0.105	0.241	1.14 (CN)	−0.99 (BF_3)
BP86	−0.005	0.215	1.21 (CN)	−0.89 (BF_3)
PW91	−0.047	0.221	1.19 (CN)	−0.92 (BF_3)
PBE	−0.105	0.235	1.11 (CN)	−1.01 (BF_3)
HCTH	0.043	0.232	1.34 (CN)	−0.87 (B_2F_4)
OLYP	−0.231	0.288	0.99 (CN)	−1.11 (BF_3)
B3LYP	0.009	0.184	1.57 (CN)	−0.57 (B_2F_4)
B3PW91	−0.012	0.190	1.58 (CN)	−0.65 (B_2F_4)
B3P86	0.550	0.551	2.13 (CN)	−0.07 (B_2F_4)
PBE0	−0.064	0.199	1.61 (CN)	−0.67 (B_2F_4)
VSXC	−0.103	0.226	1.20 (CN)	−0.88 (BF_3)
PKZB	−0.276	0.310	0.88 (CN)	−1.31 (BF_3)
TPSS	−0.134	0.242	1.22 (CN)	−1.02 (BF_3)
TPSSh	−0.113	0.229	1.41 (CN)	−0.79 (BF_3)

TABLE III. Summary of deviations from experiment of electron affinities (EAs) of the G3/99 test set (58 species) computed using the 6-311++G($3df,3pd$) basis. The geometries and zero-point energies were obtained at the B3LYP/6-31G($2df,p$) level using a frequency scale factor of 0.9854. All values are in eV. Error=theory−experiment. The mean experimental EA is 1.41 eV.

Method	ME	MAE	Max (+)	Max (−)
HF	−1.033	1.101	1.28 (C_2)	−2.21 (F)
LSDA	0.234	0.244	0.88 (C_2)	−0.15 (NO_2)
BLYP	0.008	0.115	0.70 (C_2)	−0.26 (NCO)
BPW91	0.035	0.119	0.78 (C_2)	−0.31 (NO_2)
BP86	0.178	0.190	0.89 (C_2)	−0.15 (NO_2)
PW91	0.109	0.138	0.84 (C_2)	−0.21 (NO_2)
PBE	0.061	0.118	0.78 (C_2)	−0.29 (NO_2)
HCTH	0.148	0.187	0.90 (C_2)	−0.27 (PH)
OLYP	−0.115	0.148	0.60 (C_2)	−0.47 (NO_2)
B3LYP	0.088	0.124	1.10 (C_2)	−0.09 (HOO)
B3PW91	0.031	0.137	1.08 (C_2)	−0.26 (HOO)
B3P86	0.587	0.587	1.63 (C_2)	None
PBE0	−0.027	0.165	1.09 (C_2)	−0.39 (HOO)
VSXC	−0.015	0.128	0.78 (C_2)	−0.35 (NO_2)
PKZB	−0.116	0.153	0.57 (C_2)	−0.51 (NO_2)
TPSS	−0.020	0.137	0.82 (C_2)	−0.32 (NO_2)
TPSSh	−0.046	0.164	0.95 (C_2)	−0.33 (HOO)

on the G3-3 set. Note also that the OLYP functional, whose exchange component[39] was designed as a refinement of the B88 exchange,[5] does perform considerably better than BLYP for systems of light atoms ($Z \leqslant 18$). The highly parametrized HCTH/407,[11] however, is not as accurate as one might have expected.

B. Ionization potentials

The G2/97 and G3/99 test sets contain 88 ionization potentials (IPs) for systems built from atoms of atomic number 18 or less. Since the $^2A_1$ excited state of H_2S^+ and the $^2\Pi$ excited state of N_2^+ do not converge in nonhybrid DFT methods,[55] we dropped them leaving a total of 86 ionized molecules and atoms. In this set, all ions and neutrals are in their ground states. Following Curtiss et al.,[55] IPs were evaluated as the difference in total energies at 0 K of the cation and the corresponding neutral, at their respective B3LYP/6-31G($2df,p$) geometries using scaled B3LYP/6-31G($2df,p$) ZPEs.

Table II shows that, except for B3P86 (MAE $=0.55$ eV), all functionals give mean absolute deviations between 0.2 and 0.3 eV. This does not hide the fact that TPSS (ME$=-0.13$ eV) has a much weaker tendency to underestimate IPs than PKZB (ME$=-0.28$ eV) and, as a result, yields a significantly smaller MAE (0.24 eV as opposed to 0.31 eV for PKZB). The MAE of TPSS is comparable to that of most other GGA, hybrid GGA, and MGGA functionals. In agreement with the observation made by Ernzerhof and Scuseria,[42] GGAs and MGGAs fail to reduce the LSDA error for ionization potentials. With the exception of B3P86, hybrids perform better than the corresponding nonhybrid functionals. The largest deviations with all functionals occur for the CN molecule because the open-shell singlet state of the CN^+ ion ($^1\Sigma^+$) poses a problem for DFT.[55]

Inadequacy of approximate density functionals is not the only source of errors. As shown by Baboul et al.,[61] the B3LYP method gives poor geometries for several cations of the IP test set. In particular, the equilibrium B3LYP structure of CH_4^+ has a D_{2d} symmetry instead of the correct C_{2v}, BCl_3^+ is D_{3h} instead of C_{2v}, and BF_3^+ (C_{2v}) has severely distorted bond lengths. Unreasonably large deviations for CH_4^+, BF_3^+, and BCl_3^+, predicted with nearly all functionals, are thus artifacts.

C. Electron affinities

Negative ions are actually unstable within approximate DFT models that are not completely free from self-interaction. This applies to all present-day functionals. Positive values of electron affinities (EAs) that are routinely obtained in practice are due to the artificial stabilization of anions by finite basis sets.[64] It is clear that the success or failure of a particular density functional for EAs depends not so much on the quality of the functional itself as on cancellation of errors and basis set effects. Nevertheless, since we explore not just density functionals but ''model chemistries,'' it is not unreasonable to include EAs in our tests.

We evaluated electron affinities as the difference between the total energies at 0 K of the anion and the corresponding neutral, at their respective B3LYP/6-31G($2df,p$) geometries. The results appear in Table III. As with IPs, there are no large variations in performance between various functionals. Only B3P86 and LSDA have anomalously high (overbinding) errors, and just two functionals, OLYP and PKZB, show appreciable underbinding. The MAE of TPSS (0.14 eV) is a little smaller than that of PKZB (0.15 eV). However, TPSS entirely eliminates the tendency of PKZB to underbind the added electron. The reasons[44,65] that make hybrid functionals so successful for atomization energies do not

TABLE IV. Summary of deviations from experiment of proton affinities (PAs) for the eight molecules of the G3/99 test set computed using the $6\text{-}311++G(3df,3pd)$ basis. The geometries and zero-point energies were obtained at the B3LYP/6-31G($2df,p$) level using a frequency scale factor of 0.9854. All values are in eV. Error=theory−experiment. The mean experimental PA is 158.0 kcal/mol.

Method	ME	MAE	Max (+)	Max (−)
HF	1.82	3.14	6.9 (PH$_3$)	−2.6 (H$_2$)
LSDA	−5.90	5.90	None	−10.6 (PH$_3$)
BLYP	−1.46	1.57	0.4 (C$_2$H$_2$)	−3.9 (H$_2$O)
BPW91	0.86	1.45	3.8 (C$_2$H$_2$)	−1.3 (PH$_3$)
BP86	−0.45	1.33	2.4 (C$_2$H$_2$)	−2.9 (PH$_3$)
PW91	−0.85	1.58	2.2 (C$_2$H$_2$)	−3.5 (PH$_3$)
PBE	−0.82	1.60	2.4 (C$_2$H$_2$)	−3.6 (PH$_3$)
HCTH	1.94	1.94	5.3 (C$_2$H$_2$)	None
OLYP	1.52	1.73	5.4 (C$_2$H$_2$)	−0.6 (H$_2$O)
B3LYP	−0.77	1.16	1.6 (C$_2$H$_2$)	−2.3 (H$_2$)
B3PW91	0.97	1.07	4.2 (C$_2$H$_2$)	−0.3 (SiH$_4$)
B3P86	0.49	0.99	3.5 (C$_2$H$_2$)	−0.9 (SiH$_4$)
PBE0	0.18	1.14	3.9 (C$_2$H$_2$)	−1.7 (SiH$_4$)
VSXC	0.99	1.59	5.0 (C$_2$H$_2$)	−1.5 (H$_2$)
PKZB	1.33	1.80	6.5 (C$_2$H$_2$)	−0.8 (H$_2$O)
TPSS	1.68	1.82	4.4 (C$_2$H$_2$)	−0.5 (H$_2$O)
TPSSh	1.77	1.77	4.8 (C$_2$H$_2$)	None

apply to ionization and electron addition. This is why the mixing of DFT and exact exchange is actually counterproductive for electron affinities (e.g., the MAE of TPSSh increases to 0.16 eV). The open-shell singlet C$_2$ ($^1\Sigma_g^+$) molecule, which is isoelectronic with CN$^+$ ($^1\Sigma^+$), poses a symmetry dilemma for single-determinantal methods,[66–68] with the result that the EA of C$_2$ has the largest positive deviation from experiment for all methods.

D. Proton affinities

The eight proton affinities (PAs) included in the G3/99 test set were computed as the differences between the energies of neutral and protonated molecules in their lowest vibrational states, PA(M)=E_0(M)−E_0(MH$^+$). As usual, we used the geometries and scaled frequencies obtained at the B3LYP/6-31G($2df,p$) level. Addition of a proton to a neutral molecule does not change the number of electrons but alters the geometry and causes a redistribution of the electron density. The process is accompanied by an increase (in absolute value) of exchange and correlation energies. This effect is best captured by hybrid density functionals which yield PAs with an average error of about 1 kcal/mol (see Table IV). GGA functionals are less accurate, followed by MGGAs. Proton affinity is the only property tested for which the TPSS functional shows no gain in accuracy over PKZB. Note also that LSDA underbinds the proton and HF overbinds, reversing the trends which these two methods exhibit for enthalpies of formation, IPs, and EAs.

V. BOND LENGTHS

To probe the predictive power of the TPSS functional for molecular geometries, we compiled a test set of 96 ground-state molecules with well-established equilibrium internuclear distances (r_e). This set, referred to as T-96R, combines

TABLE V. Specification of the T-96R test set for bond length calculations. Experimental equilibrium bond lengths are taken from Ref. 75 (all neutrals except Be$_2$), Ref. 76 (cations), and Ref. 77 (Be$_2$).

H$_2$, Li$_2$, LiH, LiF, LiCl, LiO, Be$_2$, BeH, BeF, BeO, BeS, B$_2$, BH, BF, BF$_3$, BCl, BCl$_3$, BN, BO, BS, C$_2$ ($^1\Sigma_g^+$), CH, CH$_4$, CF, CF$_4$, CCl, CCl$_4$, CN, CO, CO$^+$, CO$_2$, CP, CS, CS$_2$, N$_2$, N$_2^+$, NH, NH$^+$, NF, NCl, NO, NO$^+$, NS, O$_2$, O$_2^+$, OH, OH$^+$, OF, F$_2$, F$_2^+$, HF, HF$^+$, Na$_2$, NaH, NaF, NaCl, NaO, MgH, MgF, MgCl, MgO, Al$_2$, AlH, AlF, AlCl, AlO, AlS, Si$_2$, SiH, SiH$_4$, SiF, SiF$_4$, SiCl, SiCl$_4$, SiN, SiO, SiS, P$_2$, P$_4$, PH, PF, PCl, PN, PO, S$_2$, SH, SF, SF$_6$, SO, SO$_3$, Cl$_2$, Cl$_2^+$, HCl, HCl$^+$, ClF, ClO

86 neutral molecules and 10 molecular cations (for a complete list see Table V). The subset of neutral species includes most of the observable diatomic molecules built up from atoms H through Cl as well as several polyatomic molecules of high symmetry whose geometry is completely determined by a single bond length. All geometry optimizations were carried out using the $6\text{-}311++G(3df,3pd)$ basis with the options Opt=Tight and Int(Grid=UltraFine).

Improvement of PKZB geometries within the MGGA framework was one of the principal motivations for the development of the TPSS functional. Table VI shows that this goal has been fully accomplished. The bond length MAE of TPSS (0.014 Å) is only half as large as that of PKZB (MAE=0.027 Å) and smaller than for any GGA functional. Note that LSDA (the first rung of Jacob's ladder) gives more accurate bond lengths than any functional of the second rung. Inclusion of exact exchange has a remedial effect on bond lengths: the smallest errors in Table VI are associated with hybrid functionals, all of which have a MAE of about 0.01 Å. The largest individual deviations are observed, as

TABLE VI. Summary of deviations from experiment of equilibrium bond lengths (r_e) for 96 diatomic molecules of the T-96R test set computed using the $6\text{-}311++G(3df,3pd)$ basis. All values are in Å. Error=theory −experiment. The mean experimental r_e is 1.565 Å.

Method	ME	MAE	Max (+)	Max (−)
HF[a]	−0.0105	0.0249	0.115 (Na$_2$)	−0.112 (F$_2^+$)
LSDA[b]	0.0005	0.0131	0.042 (BN)	−0.094 (Na$_2$)
BLYP	0.0212	0.0223	0.055 (Al$_2$)	−0.032 (Na$_2$)
BPW91	0.0166	0.0168	0.070 (Li$_2$)	−0.007 (F$_2^+$)
BP86	0.0174	0.0175	0.060 (Li$_2$)	−0.006 (F$_2^+$)
PW91	0.0139	0.0145	0.054 (Li$_2$)	−0.016 (Be$_2$)
PBE	0.0153	0.0159	0.055 (Li$_2$)	−0.013 (Be$_2$)
HCTH	0.0089	0.0145	0.086 (Na$_2$)	−0.087 (Si$_2$)
OLYP	0.0168	0.0177	0.103 (Na$_2$)	−0.017 (F$_2^+$)
B3LYP	0.0050	0.0104	0.041 (Be$_2$)	−0.040 (Na$_2$)
B3PW91	0.0026	0.0093	0.060 (Li$_2$)	−0.042 (F$_2^+$)
B3P86	−0.0004	0.0084	0.038 (Be$_2$)	−0.044 (F$_2^+$)
PBE0	−0.0006	0.0097	0.063 (Be$_2$)	−0.052 (F$_2^+$)
VSXC	0.0116	0.0131	0.085 (Na$_2$)	−0.023 (P$_4$)
PKZB	0.0267	0.0269	0.145 (Na$_2$)	−0.005 (F$_2^+$)
TPSS	0.0138	0.0142	0.078 (Li$_2$)	−0.008 (P$_4$)
TPSSh	0.0075	0.0101	0.074 (Li$_2$)	−0.026 (F$_2^+$)

[a]Does not include Be$_2$ (unbound).
[b]Does not include F$_2^+$ and SF (fails to converge).

J. Chem. Phys., Vol. 119, No. 23, 15 December 2003

Nonempirical DFT   12135

TABLE VII. Specification of the T-82F test set for vibrational frequency calculations. Experimental harmonic frequencies are taken from Ref. 75 (all neutrals except LiNa and Be$_2$), Ref. 76 (LiNa and cations), and Ref. 77 (Be$_2$).

H$_2$, Li$_2$, LiH, LiF, LiCl, LiO, LiNa, Be$_2$, BeH, BeH$^+$, BeF, BeCl, BeO, BeS, B$_2$, BH, BF, BCl, BN, BO, BS, C$_2$ ($^1\Sigma_g^+$), CH, CF, CN, CO, CO$^+$, CP, CS, N$_2$, N$_2^+$, NH, NF, NCl, NO, NO$^+$, NS, O$_2$, O$_2^+$, OH, OH$^+$, F$_2$, F$_2^+$, HF, HF$^+$, Na$_2$, NaH, NaF, NaO, MgH, MgH$^+$, MgO, MgS, Al$_2$, AlH, AlF, AlCl, AlO, AlS, Si$_2$, SiH, SiH$^+$, SiF, SiCl, SiN, SiO, SiS, P$_2$, P$_2^+$, PH, PF, PCl, PN, PO, S$_2$, SO, Cl$_2$, Cl$_2^+$, HCl, HCl$^+$, ClF, ClO

one would expect, for weakly bound molecules, such as F$_2^+$, and metal dimers.

VI. VIBRATIONAL FREQUENCIES

Experimental harmonic vibrational frequencies (ω_e) are readily available for many diatomic and a few polyatomic molecules. (Not a direct observable, ω_e is the frequency that would arise in the harmonic approximation at 0 K, other effects having been taken into account in the analysis of the experiment). We have compiled a test set of 82 ground-state diatomic molecules with well-known ω_e values (see Table VII). The set, called T-82F, combines 69 neutrals and 13 cations in their ground states. The neutral subset includes most of the observable diatomic molecules of first- and second-row elements. All frequencies were computed at the respective equilibrium geometries using the 6-311+ +G($3df,3pd$) basis and the UltraFine grid.

Table VIII shows that all nonhybrid functionals underestimate vibrational frequencies. A 10%–25% contribution of exact exchange is sufficient to reverse the trend. In agreement with the study of Adamo et al.,[30] we find that the

TABLE VIII. Summary of deviations from experiment of harmonic vibrational frequencies (ω_e) for 82 diatomic molecules of the T-82F test set computed using the 6-311++G($3df,3pd$) basis. All values are in cm^{-1}. Error=theory−experiment. The mean experimental ω_e is 1429.5 cm^{-1}.

Method	ME	MAE	Max (+)	Max (−)
HF[a]	109.4	136.2	596.1 (O$_2^+$)	−272.0 (NS)
LSDA[b]	−11.8	48.9	140.7 (F$_2$)	−227.7 (H$_2$)
BLYP	−51.1	55.2	66.9 (Be$_2$)	−224.3 (HF$^+$)
BPW91	−32.6	41.4	72.1 (Be$_2$)	−161.7 (HF$^+$)
BP86	−37.7	45.5	71.4 (F$_2^+$)	−180.4 (HF$^+$)
PW91	−29.3	39.8	82.1 (Be$_2$)	−170.1 (HF$^+$)
PBE	−31.7	42.0	82.5 (Be$_2$)	−175.3 (HF$^+$)
HCTH	−14.6	39.9	115.7 (O$_2^+$)	−116.9 (MgH)
OLYP	−28.7	40.2	89.4 (F$_2^+$)	−123.7 (OH$^+$)
B3LYP	9.5	33.5	161.9 (F$_2^+$)	−99.2 (HF$^+$)
B3PW91	21.9	36.2	194.0 (F$_2^+$)	−51.6 (HF$^+$)
B3P86	26.9	37.0	201.0 (F$_2^+$)	−52.3 (HF$^+$)
PBE0	34.7	43.6	236.3 (O$_2^+$)	−36.2 (AlH)
VSXC	−12.2	33.9	100.3 (N$_2^+$)	−162.1 (BeH)
PKZB	−45.6	51.7	70.5 (F$_2^+$)	−162.8 (BH)
TPSS	−18.7	30.4	81.2 (F$_2^+$)	−145.9 (HF)
TPSSh	5.6	26.9	151.3 (F$_2^+$)	−73.7 (HF)

[a]Does not include Be$_2$ (unbound).
[b]Does not include F$_2^+$ (fails to converge).

TABLE IX. Summary of deviations from MP2(full) of dissociation energies (D_0) and selected equilibrium structural parameters (11 H-bond lengths and 13 bond angles) of 10 hydrogen-bonded complexes computed using the 6-311++G($3df,3pd$) basis. See the text and Ref. 51 for details. Error =theory−MP2. The mean MP2 D_0, H-bond length, and angle are 13.4 kcal/mol, 2.062 Å, and 111.4°, respectively.

Method	D_0 (kcal/mol)		Bond lengths (Å)		Angles (deg)	
	ME	MAE	ME	MAE	ME	MAE
HF	−2.77	2.77	0.139	0.160	−0.25	4.15
LSDA	5.78	5.78	−0.127	0.147	−0.55	4.02
BLYP	−0.46	0.64	0.027	0.034	−0.09	1.63
BPW91	−0.69	0.99	0.008	0.045	−0.14	2.08
BP86	0.08	0.76	−0.014	0.040	−0.21	2.48
PW91	1.41	1.43	−0.028	0.052	−0.30	2.55
PBE	0.94	1.00	−0.018	0.043	−0.25	2.55
HCTH	−0.91	0.91	0.078	0.084	0.11	1.42
OLYP	−2.18	2.18	0.136	0.157	0.43	1.20
B3LYP	−0.29	0.43	0.017	0.017	−0.10	1.12
B3PW91	−0.50	0.88	0.005	0.035	−0.08	1.52
B3P86	0.35	0.73	−0.023	0.043	−0.18	1.87
PBE0	0.48	0.66	−0.012	0.032	−0.16	1.84
VSXC	−0.96	1.34	0.071	0.116	−2.75	18.77
PKZB	−2.90	2.90	0.179	0.179	−0.21	3.47
TPSS	0.25	0.59	−0.006	0.021	−0.25	2.02
TPSSh	0.70	0.78	−0.002	0.015	−0.25	1.66

PKZB approximation is not competitive for vibrational frequencies. In our table, PKZB ranks second from the bottom after BLYP in terms of accuracy. The improvement from PKZB to TPSS is so significant that the TPSS functional becomes more accurate than all tested approximations other than TPSSh. Inclusion of exact exchange causes a further increase in accuracy, making TPSSh the only functional with a MAE of less than 30 cm^{-1}.

VII. HYDROGEN-BONDED COMPLEXES

Accurate description of weakly bonded systems is requisite in applications to biologically important molecules. Practical density functionals have been variably successful in describing hydrogen-bonded complexes.[69] Our test set contains ten hydrogen-bonded complexes used earlier for an assessment of the VSXC and PKZB functionals by Rabuck and Scuseria.[31] It includes (HF)$_2$, (HCl)$_2$, (H$_2$O)$_2$, HF/HCN, HF/H$_2$O, CN$^-$/H$_2$O OH$^-$/H$_2$O, HCC$^-$/H$_2$O, H$_3$O$^+$/H$_2$O, and NH$_4^+$/H$_2$O. We employed the 6-311++G($3df,3pd$) basis to optimize the geometries with each functional and evaluated ZPE corrections using unscaled frequencies. Table IX reports statistical summaries for calculations of the dissociation energies (D_0) and selected structural parameters (11 H-bonds and 13 characteristic angles). With two exceptions, the latter are the same as the parameters reported by Rabuck and Scuseria.[31] (We fixed the angle α in HF/HCN at 180° and added the O–H bond of the O–H$\cdots$O bridge in the OH$^-$/H$_2$O complex.) For lack of reliable experimental data for several complexes, we used the MP2(full)/6-311+ +G($3df,3pd$) dissociation energies and equilibrium geometries as a reference, since they agree with available experimental D_0, r_e, and bond angles.[51] Also, since the 6-311+

+G($3df,3pd$) basis is fairly large, we did not include basis set superposition error corrections in D_0 values.

According to Table IX, TPSS emerges as the most reliable nonhybrid functional for dissociation energies and geometries of H-bonded systems. It also represents a dramatic improvement over PKZB. The hybrid functionals are more accurate than their nonhybrid counterparts, although TPSSh surpasses TPSS only for geometries.

Note that the MAE of bond angles for VSXC is much greater than for any other method. This occurs because the equilibrium VSXC/6-311++G($3df,3pd$) structures of $(HF)_2$ and $(HCl)_2$ have C_{2h} symmetry rather than the correct C_s. Interestingly, the transition from C_s to C_{2h} symmetry does not occur if one uses a basis set with fewer polarization functions. This explains why our MAE for VSXC bond angles is so different from the value reported by Rabuck and Scuseria,[31] who used the 6-311++G(d,p) basis.

Another interesting observation is that not all methods predict unequal lengths for the two O–H bonds of the O–H···O bridge in the OH^-/H_2O complex. Those that do so include HF, BLYP, B3LYP, HCTH, VSXC, PKZB, TPSS, TPSSh, and MP2.

VIII. CONCLUSIONS

The TPSS MGGA is generally superior to all previously designed nonempirical functionals. Specifically, TPSS is much more accurate than LSDA and the PBE GGA for enthalpies of formation, vibrational frequencies, and hydrogen bonds. The problems of the PKZB MGGA (overestimated bond lengths, poor frequencies, and inaccurate geometries of H-bonds) have all been resolved. We attribute the progress from PKZB to TPSS to the elimination of divergence of the exchange potential at the nucleus and the satisfaction of additional exact constraints.[32] What is more, our new MGGA and its hybrid version, TPSSh, approach and in some cases surpass in accuracy the best available semiempirical approximations such as B3LYP, B3PW91, and VSXC.

Semiempirical density functionals rarely deliver a consistently strong performance. For instance, B3P86 is unrivaled for bond lengths but is the worst performer for ionization potentials and electron affinities; VSXC is superb for atomization energies and other molecular properties, but is a relative failure for systems held together by hydrogen bonds; B3LYP is good for almost any property when applied to small molecules, but yields to less "popular" functionals as molecules increase in size. In contrast, sophisticated nonempirical functionals should provide a *uniformly accurate* description of diverse systems and properties, putting to rest the "different functionals for different tasks" philosophy. In the tests we have made here for molecules and complexes and in Ref. 33 for solids and surfaces, TPSS does in fact provide such a description, although further tests (e.g., for transition elements[70]) remain to be done. One should not necessarily expect accurate results for van der Waals systems[71] from any functionals on the first four rungs of Jacob's ladder. Since TPSS has the same large-gradient behavior as PBE, it is expected[33] to perform like PBE for such systems.

The flaws remaining in the TPSS approximation (the most pressing of which is the self-interaction error in the exchange) can be dealt with by introducing a self-interaction-free local hybrid functional.[16,72] But that goes beyond the scope of MGGA and brings us to the fourth rung of the ladder.

ACKNOWLEDGMENTS

[1] W. Kohn and L. J. Sham, Phys. Rev. **140**, A1133 (1965).

[2] R. G. Parr and W. Yang, *Density-Functional Theory of Atoms and Molecules* (Oxford University Press, New York, 1989).

[3] R. M. Dreizler and E. K. U. Gross, *Density Functional Theory* (Springer, Berlin, 1990).

[4] *A Primer in Density Functional Theory*, edited by C. Fiolhais, F. Nogueira, and M. Marques (Springer, Berlin, 2003).

[5] A. D. Becke, Phys. Rev. A **38**, 3098 (1988).

[6] C. Lee, W. Yang, and R. G. Parr, Phys. Rev. B **37**, 785 (1988); B. Miehlich, A. Savin, H. Stoll, and H. Preuss, Chem. Phys. Lett. **157**, 200 (1989).

[7] P. J. Stephens, F. J. Devlin, C. F. Chabalowski, and M. J. Frisch, J. Phys. Chem. **98**, 11623 (1994); see also R. H. Hertwig and W. Koch, Chem. Phys. Lett. **268**, 345 (1997) concerning the parametrization of B3LYP.

[8] A. D. Becke, J. Chem. Phys. **107**, 8554 (1997).

[9] H. L. Schmider and A. D. Becke, J. Chem. Phys. **108**, 9624 (1998).

[10] F. A. Hamprecht, A. J. Cohen, D. J. Tozer, and N. C. Handy, J. Chem. Phys. **109**, 6264 (1998).

[11] A. D. Boese and N. C. Handy, J. Chem. Phys. **114**, 5497 (2001).

[12] T. Van Voorhis and G. E. Scuseria, J. Chem. Phys. **109**, 400 (1998).

[13] H. L. Schmider and A. D. Becke, J. Chem. Phys. **109**, 8188 (1998).

[14] A. D. Boese and N. C. Handy, J. Chem. Phys. **116**, 9559 (2002).

[15] G. K.-L. Chan and N. C. Handy, J. Chem. Phys. **112**, 5639 (2000).

[16] J. P. Perdew and K. Schmidt, in *Density Functional Theory and Its Application to Materials*, edited by V. Van Doren, C. Van Alsenoy, and P. Geerlings (AIP, Melville, New York, 2001).

[17] A. E. Mattsson, Science **298**, 759 (2002).

[18] S. H. Vosko, L. Wilk, and M. Nusair, Can. J. Phys. **58**, 1200 (1980).

[19] J. P. Perdew and Y. Wang, Phys. Rev. B **45**, 13244 (1992).

[20] J. P. Perdew, K. Burke, and M. Ernzerhof, Phys. Rev. Lett. **77**, 3865 (1996); **78**, 1396 (1997)(E)).

[21] J. P. Perdew, K. Burke, and Y. Wang, Phys. Rev. B **54**, 16533 (1996).

[22] J. P. Perdew, Phys. Rev. Lett. **55**, 1665 (1985).

[23] S. K. Ghosh and R. G. Parr, Phys. Rev. A **34**, 785 (1986).

[24] A. D. Becke and M. R. Roussel, Phys. Rev. A **39**, 3761 (1989).

[25] M. Filatov and W. Thiel, Phys. Rev. A **57**, 189 (1998).

[26] J. P. Perdew, S. Kurth, A. Zupan, and P. Blaha, Phys. Rev. Lett. **82**, 2544 (1999).

[27] J. B. Krieger, J. Chen, G. J. Iafrate, and A. Savin, in *Electron Correlations and Materials Properties*, edited by A. Gonis, N. Kioussis, and M. Ciftan (Kluwer/Plenum, New York, 1999); J. Toulouse, A. Savin, and C. Adamo, J. Chem. Phys. **117**, 10465 (2002).

[28] E. Proynov, H. Chermette, and D. R. Salahub, J. Chem. Phys. **113**, 10013 (2000).

[29] S. Kurth, J. P. Perdew, and P. Blaha, Int. J. Quantum Chem. **75**, 889 (1999).

[30] C. Adamo, M. Ernzerhof, and G. E. Scuseria, J. Chem. Phys. **112**, 2643 (2000).

[31] A. D. Rabuck and G. E. Scuseria, Theor. Chem. Acc. **104**, 439 (2000).

[32] J. Tao, J. P. Perdew, V. N. Staroverov, and G. E. Scuseria, Phys. Rev. Lett. **91**, 146401 (2003).

[33] V. N. Staroverov, G. E. Scuseria, J. Tao, and J. P. Perdew (unpublished).

[34] P. J. Feibelman, Science **295**, 99 (2002).

[35] A. D. Becke, J. Chem. Phys. **104**, 1040 (1996).

J. Chem. Phys., Vol. 119, No. 23, 15 December 2003

Nonempirical DFT   12137

[36] J. P. Perdew, in *Electronic Structure of Solids*, edited by P. Ziesche and H. Eschrig (Akademie, Berlin, 1991).

[37] J. P. Perdew, J. A. Chevary, S. H. Vosko, K. A. Jackson, M. R. Pederson, D. J. Singh, and C. Fiolhais, Phys. Rev. B **46**, 6671 (1992).

[38] J. P. Perdew, Phys. Rev. B **33**, 8822 (1986).

[39] N. C. Handy and A. J. Cohen, Mol. Phys. **99**, 403 (2001).

[40] A. D. Becke, J. Chem. Phys. **98**, 5648 (1993).

[41] M. J. Frisch *et al.* (unpublished). Implemented in the GAUSSIAN program. B3P86 is identical to B3PW91 except that it replaces the LSDA correlation parametrization of Ref. 19 by Eq. (3.1) of Ref. 18 and the PW91 gradient correction for correlation by the gradient correction of the 1986 Perdew correlation functional (P86)—Ref. 38. Like B3LYP (Ref. 7) and unlike B3PW91 or BP86, B3P86 has a local correlation term that is not exact. Instead, the B3P86 local correlation term is evaluated in the random phase approximation (RPA) option of Ref. 18, while that of B3LYP is 81% RPA and 19% LYP.

[42] M. Ernzerhof and G. E. Scuseria, J. Chem. Phys. **110**, 5029 (1999).

[43] C. Adamo and V. Barone, J. Chem. Phys. **110**, 6158 (1999).

[44] J. P. Perdew, M. Ernzerhof, and K. Burke, J. Chem. Phys. **105**, 9982 (1996).

[45] F. Jensen, J. Chem. Phys. **116**, 7372 (2002); **118**, 2459 (2003).

[46] A. D. Boese, J. M. L. Martin, and N. C. Handy, J. Chem. Phys. **119**, 3005 (2003).

[47] M. J. Frisch *et al.*, GAUSSIAN Development Version, Revision B.01, Gaussian, Inc., Pittsburgh, PA (2003).

[48] R. Neumann, R. H. Nobes, and N. C. Handy, Mol. Phys. **87**, 1 (1996).

[49] J. F. Dobson, J. Phys.: Condens. Matter **4**, 7877 (1992).

[50] S. Kümmel and J. P. Perdew, Phys. Rev. Lett. **90**, 043004 (2003).

[51] See EPAPS Document No. E-JCPSA6-119-302348 for our detailed results for individual molecules and complexes. A direct link to this document may be found in the online article's HMTL reference section. The document may be also retrieved via the EPAPS homepage (http://www.aip.org/pubservs/epaps.html) or from ftp.aip.org in the directory /epaps/. See the EPAPS homepage for more information.

[52] J. A. Pople, M. Head-Gordon, D. J. Fox, K. Raghavachari, and L. A. Curtiss, J. Chem. Phys. **90**, 5622 (1989).

[53] L. A. Curtiss, C. Jones, G. W. Trucks, K. Raghavachari, and J. A. Pople, J. Chem. Phys. **93**, 2537 (1990).

[54] L. A. Curtiss, K. Raghavachari, P. C. Redfern, and J. A. Pople, J. Chem. Phys. **106**, 1063 (1997).

[55] L. A. Curtiss, P. C. Redfern, K. Raghavachari, and J. A. Pople, J. Chem. Phys. **109**, 42 (1998).

[56] L. A. Curtiss, K. Raghavachari, P. C. Redfern, and J. A. Pople, J. Chem. Phys. **112**, 7374 (2000).

[57] L. A. Curtiss, K. Raghavachari, G. W. Trucks, and J. A. Pople, J. Chem. Phys. **94**, 7221 (1991).

[58] L. A. Curtiss, K. Raghavachari, P. C. Redfern, V. Rassolov, and J. A. Pople, J. Chem. Phys. **109**, 7764 (1998).

[59] C. W. Bauschlicher and H. Partridge, J. Chem. Phys. **103**, 1788 (1995).

[60] A. M. Mebel, K. Morokuma, and M. C. Lin, J. Chem. Phys. **103**, 7414 (1995).

[61] A. G. Baboul, L. A. Curtiss, P. C. Redfern, and K. Raghavachari, J. Chem. Phys. **110**, 7650 (1999).

[62] L. A. Curtiss, P. C. Redfern, K. Raghavachari, and J. A. Pople, J. Chem. Phys. **114**, 108 (2001).

[63] G. I. Csonka, A. Ruzsinszky, J. Tao, and J. P. Perdew (unpublished).

[64] N. Rösch and S. B. Trickey, J. Chem. Phys. **106**, 8940 (1997).

[65] K. Burke, J. P. Perdew, and M. Ernzerhof, in *Electronic Density Functional Theory: Recent Progress and New Directions*, edited by J. F. Dobson, G. Vignale, and M. P. Das (Plenum, New York, 1998).

[66] A. Goursot, J. P. Malrieu, and D. R. Salahub, Theor. Chim. Acta **91**, 225 (1995).

[67] P. R. T. Schipper, O. V. Gritsenko, and E. J. Baerends, Theor. Chem. Acc. **99**, 329 (1998).

[68] A. von Kopylow and D. Kolb, Chem. Phys. Lett. **295**, 439 (1998).

[69] H. Guo, S. Sirois, E. I. Proynov, and D. R. Salahub, in *Theoretical Treatment of Hydrogen Bonding*, edited by D. Hadzi (Wiley, Chichester, 1997).

[70] F. Furche (unpublished).

[71] H. Rydberg, M. Dion, N. Jacobson, E. Schröder, P. Hyldgaard, S. I. Simak, D. C. Langreth, and B. I. Lundqvist, Phys. Rev. Lett. **91**, 126402 (2003).

[72] J. Jaramillo, G. E. Scuseria, and M. Ernzerhof, J. Chem. Phys. **118**, 1068 (2003).

[73] J. P. Perdew, R. G. Parr, M. Levy, and J. L. Balduz, Jr., Phys. Rev. Lett. **49**, 1691 (1982).

[74] E. Clementi and C. Roetti, At. Data Nucl. Data Tables **14**, 177 (1974).

[75] *CRC Handbook of Chemistry and Physics*, edited by D. R. Lide, 83rd ed. (CRC, Boca Raton, FL, 2002).

[76] K. P. Huber and G. Herzberg, *Molecular Spectra and Molecular Structure. IV. Constants of Diatomic Molecules* (Van Nostrand, New York, 1979).

[77] J. M. L. Martin, Chem. Phys. Lett. **303**, 399 (1999).